# "Helter-Skelter-Like" Perylene Polyisocyanopeptides

**ARTICLE** *in* CHEMISTRY - A EUROPEAN JOURNAL · FEBRUARY 2009

Impact Factor: 5.73 · DOI: 10.1002/chem.200801746 · Source: PubMed

CHEMISTRY
A EUROPEAN JOURNAL

DOI: 10.1002/chem.200801746

# "Helter-Skelter-Like" Perylene Polyisocyanopeptides

Erik Schwartz,[a] Vincenzo Palermo,[b] Chris E. Finlayson,[c] Ya-Shih Huang,[c] Matthijs B. J. Otten,[a] Andrea Liscio,[b] Sara Trapani,[d] Irene González-Valls,[a] Patrick Brocorens,[d] Jeroen J. L. M. Cornelissen,[a] Kalina Peneva,[e] Klaus Müllen,[e] Frank C. Spano,[f] Arkady Yartsev,[g] Sebastian Westenhoff,[c] Richard H. Friend,*[c] David Beljonne,*[d] Roeland J. M. Nolte,[a] Paolo Samorì,*[b, h] and Alan E. Rowan*[a]

**Abstract:** We report on a combined experimental and computational investigation on the synthesis and thorough characterization of the structure of perylene-functionalized polyisocyanides. Spectroscopic analyses and extensive molecular dynamics studies revealed a well defined $4_1$ helix in which the perylene molecules form four "helter skelter-like" overlapping pathways along which excitons and electrons can rapidly migrate. The well-defined polymer scaffold stabilized by hydrogen bonding, to which the chromophores are attached, accounts for the precise architectural definition, and molecular stiffness observed for these molecules. Molecular-dynamics studies showed that the chirality present in these polymers is expressed in the formation of stable right-handed helices. The formation of chiral supramolecular structures is further supported by the measured and calculated bisignated Cotton effect. The structural definition of the chromophores aligned in one direction along the backbone is highlighted by the extremely efficient exciton migration rates and charge densities measured with Transient Absorption Spectroscopy.

**Keywords:** electron transport · perylene diimides · polyisocyanides · polymers

[a] E. Schwartz, M. B. J. Otten, I. González-Valls, Dr. J. J. L. M. Cornelissen, Prof. Dr. R. J. M. Nolte, Prof. Dr. A. E. Rowan
Institute for Molecules and Materials
Radboud University Nijmegen
Toernooiveld 1, 6525 Ed Nijmegen (The Netherlands)
Fax: (+31)-24-3652929
E-mail: a.rowan@science.ru.nl

[b] Dr. V. Palermo, Dr. A. Liscio, Prof. Dr. P. Samorì
Instituto per la Sintesi Organica e la Fotoreattività, (Institution)
Consiglio Nazional dlle Ricerche, Via Gobetti 101
40129 Bologna (Italy)
E-mail: samori@isis-ulp.org

[c] Dr. C. E. Finlayson, Y.-S. Huang, Dr. S. Westenhoff, Prof. Dr. R. H. Friend
Cavendish Laboratory, University of Cambridge
J. J. Thomson Avenue Cambridge CB3 0HE (UK)
E-mail: rhf10@cam.ac.uk

[d] S. Trapani, Dr. P. Brocorens, Dr. D. Beljonne
Université de Mons-Hainaut, Place du Parc 20
7000 Mons (Belgium)
E-mail: David@averell.umh.ac.be

[e] Dr. K. Peneva, Prof. Dr. K. Müllen
Max-Planck Institute for Polymer Research,
Ackermann 10, 55124 Mainz (Germany)

[f] Prof. Dr. F. C. Spano
Department of Chemistry, Temple University
Beury Hall 201, Philadelphia, PA 19122 (USA)

[g] Prof. A. Yartsev
Lund University
P.O. Box 124, 22100 Lund (Sweden)

[h] Prof. Dr. P. Samorì
Nanochemistry Laboratory, ISIS, Université Louis Pasteur and CNRS (UMR 7006), 8 allée Gaspard Monge
67000 Strasbourg (France)

Supporting information for this article is available on the WWW under http://dx.doi.org/10.1002/chem.200801746.

## Introduction

The synthesis of complex molecular systems ordering chromophores in well-defined positions in order to achieve extremely high energy and electron transfer pathways represents a great challenge in chemistry and materials science. This goal lies at the foundation of various optoelectronic applications, such as photovoltaic devices and field effect transistors (FETs). Within the frame of fundamental research focused on finding new systems for implementing these applications, the endeavour has been addressed towards the development of new structures featuring a cofacial arrangement of chromophores such as polycyclic aromatic systems to allow high degree of π-orbital overlap and significant exciton coupling. High electron mobilities[1,2] and also fast exciton transport over large distances[3] have been measured in such cofacial systems. Several approaches to obtain well organized perylene-bis(dicarboximides) (PDIs) structures for application in solar cells and FETs are described in the literature including studies on perylene crystals,[4–6] aggregates,[7–18] and liquid crystals.[19–21] Alongside the aggregation of monomeric PDIs units, also several examples have been reported in which face-to-face aggregation of PDIs is promoted by an oligomer or polymer architecture.[22–28] These investigations have been mainly concentrated on flexible polymers architectures. We therefore decided to investigate the incorporation of PDI units in the backbone that can adopt a very stable well-defined $4_1$ helical conformation when the side chains exhibit a bulky group or bears additional stabilizing interactions, such as π–π stacking and/or hydrogen bonding between the repeat units in the $n$ and $n+4$ positions.[29–32] The introduction of peptide substituents orders the side groups into a precise architecture, resulting in an attractive scaffold onto which functional groups can be arranged into well-defined arrays, such as thiophenes,[33] porphyrins[34] and perylenes diimides,[35,36] thus creating new materials with potentially interesting properties. Such a high order is reflected in the extraordinary high stiffness (as proven by a persistence length of 76 nm) observed by AFM measurements.[37]

These polymers could therefore be ideal candidates for photovoltaic cells, although unfortunately they suffer from a very poor solubility in organic solvents.[35,36] Moreover, the organization of the perylenes makes the material interesting for both nanoscale or macroscopic wires and field-effect transistors (FETs). In this paper we focus on the relationship between the inter-chromophore interactions in two different PDI functionalized polyisocyanopeptides and the (photophysical) properties of the material.

We report on the synthesis and characterization of two new PDI-polyisocyanide systems both having an improved solubility in organic solvents. In particular we have developed polymer **P2** exposing sterically demanding phenoxy substituents in the bay area of the PDI, and polymer **P3** bearing longer alkyl tails in the side chains of "ultra-rigid" polyisocyanides. Polyisocyanides possess a unique polymer periphery (Figure 1). The incentive to prepare and study **P2** was that the bulky phenoxy groups in the PDI bay area may hinder the well-known tendency of PDIs to stack through π–π interactions. Furthermore, the bulky character of the non-planar PDIs in **P2** may inhibit the formation of excimers, which might be beneficial for excitons transport, since excimer sites act as energy traps in which energy is lost as fluorescence. In order to achieve a thorough understanding on these three polymer systems, we combined the (photophysical) characterization in solution with an extensive modelling of the structural properties of the perylene-functionalized polymer **P3**. For the sake of comparison, polymer **P1**, which consists of a central PIC backbone exposing an alanine–alanine segment and terminal methoxy groups, was studied.

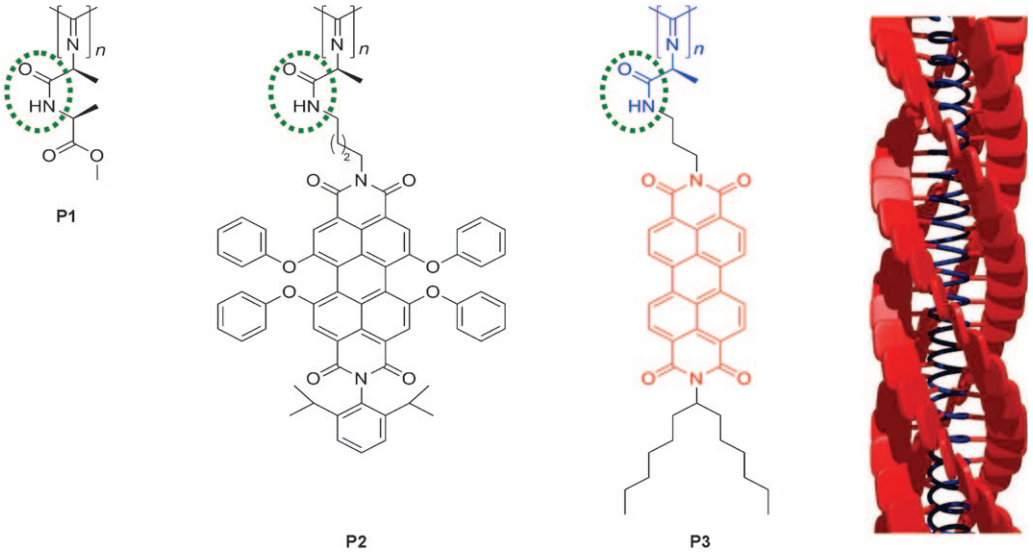


Figure 1. Molecular structure of the polymers **P1**–**P3**. The amide unit that is responsible for the stabilization of the helical structure by a hydrogen bonding network is encircled in green. A schematic structure of **P3** is depicted, with the backbone in blue and the PDI groups in red.

  

## Results and Discussion

### Synthesis of monomers and polymers

Polymers **P1**–**P3** were prepared via a nickel-catalyzed polymerization reaction of isocyanide monomers. The synthesis and characterization of polymer **P1** has been described in detail in the literature and will not be discussed here.[38] The perylene-bis(dicarboximide) functionalized polymer **P3** was synthesized following a slightly modified strategy to that described for the synthesis of PDI functionalized polyisocyanides.[35,36] First, hexylheptyl amine was treated with perylene dianhydride **1** to give the symmetrically substituted perylene diimide **2**, which after partial hydrolysis with potassium hydroxide in *tert*-butanol yielded perylene mono-anhydride **3** (Scheme 1). Subsequently **3** was functionalized with a *tert*-butyloxycarbonyl (Boc)-protected amine by reaction with mono-Boc-1,3-diaminopropane. The protected amine **4** was converted into the free amine **5** by removal of the Boc protection with an excess of trifluoroacetic acid (TFA). In the following step, amine **5** was coupled to Boc-L-alanine to give **6**, using 1-(3-dimethylaminopropyl)-3-ethylcarbodiimide hydrochloride (EDC) and hydroxybenzotriazole (HOBt) as coupling reagents. After removal of the Boc protection, amine **7** was formylated using 4-nitrophenyl formate as reagent. Dehydration of formamide **8** with diphosgene and *N*-methylmorpholine (NMM) resulted in the formation of isocyanide monomer **9**. In an analogous manner of the synthetic route from amine **5** to isocyanide **9**, the isocyanide monomer **13**, containing bulky phenoxy substituents, was prepared following the same procedure starting from amine **10** (Scheme, Supporting Information).

Isocyanide **9** was polymerized in 60 minutes using nickel complex **14** (1/1000 equiv) (Figure S2). The azide in the initiator complex **14** can be used as a possible further reaction site for modification of the polymer terminus with for example, a second polyisocyanide block or other functional groups because it ends up in the end group of the polyisocyanide, however, work in this area is not presented in this paper.

Upon polymerization of isocyanide **9**, the reaction mixture turned from yellow to red, which is a typical for the aggregation of PDIs and in this particular case indicative of the polymerization leading to intermolecular aggregation of the PDIs. The polymer was purified by repetitive precipitation; first in methanol/water (1:1 v/v) and then in methanol, until no monomer fluorescence was visible. The solubility of **P3** was found to be much better than that of the perylene functionalized polyisocyanide described in previous work,[35,36] and therefore polymer **P3** is much better process-

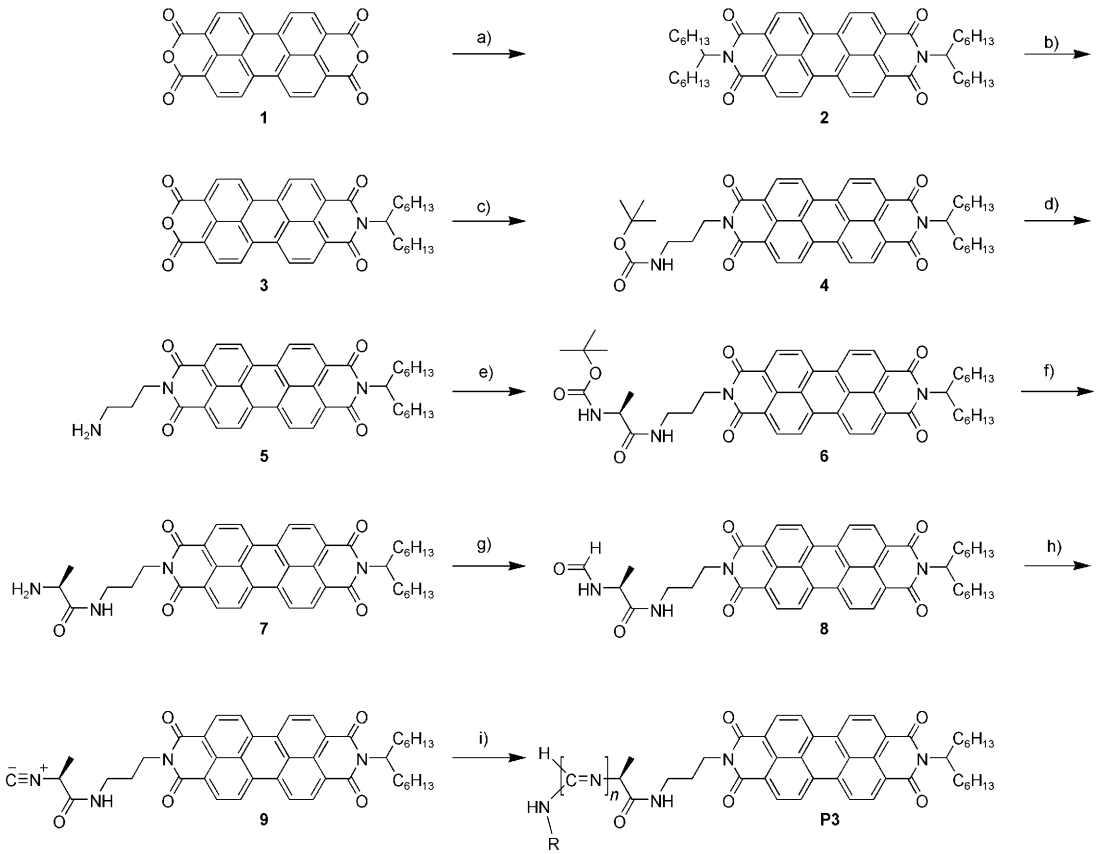


Scheme 1. Synthesis of PDI functionalized polyisocyanides **P3** ($R = CH_2CH_2CH_2N_3$). a) 1-hexylheptylamine, DMF/Imidazole, 110 °C; b) KOH, *tert*-butanol; c) Boc-1,3-diaminopropane, DMF/imidazole, 95 °C; d) TFA, $CH_2Cl_2$, quant.; e) Boc-L-alanine, EDC, HOBt, DIPEA, $CH_2Cl_2$, 67 %; f) TFA, $CH_2Cl_2$, quant.; g) 4-nitrophenyl formate, $CH_2Cl_2$, 92 %; h) diphosgene, *N*-methylmorpholine, $CH_2Cl_2$, −30 °C, 88 %; i) **14**, $CH_2Cl_2$, 98 %.

able. Polymer **P3** was soluble (to at least up to 10 mg mL$^{-1}$) in chlorinated solvents ($CH_2Cl_2$, $CHCl_3$, dichloroethane, tetrachloroethane) and solvents such as benzene, toluene and tetrahydrofuran.

In contrast to the fast polymerisation of **9**, it took seven days before monomer **13** (having phenoxy substituents) was completely consumed as was concluded from TLC analysis. This slow polymerization can be attributed to the bulkiness of the PDIs and occurs at a similar rate to that observed for the polymerization of *tert*-butyl isocyanide.[39] During the polymerization of **13** to **P2** the reaction mixture turned slightly darker, from purple to deep purple, but a clear colour change as visible in the preparation of **P3** was not observed. Polymer **P2** was purified by size-exclusion chromatography and was seen to be soluble in most organic solvents, toluene and THF. Determination of the absolute molecular weight of **P2** and **P3** using gel-permeation chromatography (GPC) is difficult because the behavior of a rod-like polymer in a gel is not straightforward. Therefore, we estimated the $M_W$s by AFM using dilute solutions of the polyisocyanide ($10^{-6}$ in $CHCl_3$) spincoated on freshly cleaved mica. This approach reveals single fibers and due to the rigidity the polymers are extended on the surface and their contour lengths can be accurately measured. This approach has been used by Prokhorova et al.[40] to determine the absolute molecular weight of polymethacrylates and polystyrenes having bulky substituents, and could be applied to our polyisocyanopeptides as well.[41] According to AFM images of **P3** on muscovite mica, the average length of **P3** is 180 nm. From the analysis of AFM images of **P2** on muscovite mica, an average polymer chain length of 110 nm was determined. Assuming a $4_1$ type helix with a helical pitch of 0.46 nm (measured by Powder X-ray diffraction of **P1**,[41,42], 180 nm corresponds to $1.2\times10^3$ repeat units and an $M_n$ value of $9\times10^5$ g mol$^{-1}$. For **P2** this leads to an $M_n$ value of $1.1\times10^6$ g mol$^{-1}$.

### Sepctroscopical methods

**Infrared spectroscopy**: To obtain greater insight into the structures of the polymers, the polymerization of **9** with catalyst **14** (1/740 equiv) was followed by IR spectroscopy (Figure S2). Most characteristic for the polymerization is the disappearance of the isocyanide peak at $\tilde{\nu}$ 2140 cm$^{-1}$ and from this signal the reaction was determined to be completely finished after ≈1000 s. Upon polymerization the absorptions at 3438 and 3391 cm$^{-1}$, attributed to the trans and *cis* amide N–H stretch vibrations, respectively,[43] shifted to 3294 cm$^{-1}$ indicative for hydrogen-bond formation of the amides, exclusively in the trans configuration. An intensity decrease at about 1686 cm$^{-1}$ and an intensity increase at about 1649 cm$^{-1}$ as observed in Figure S2 showing the difference spectrum, are ascribed to a shift of the amide I vibration (C=O stretch) due to hydrogen bonding. The slow polymerization of monomer **13** was not followed by IR spectroscopy, however, the solid-state IR spectrum of polymer **P2** compared to that of the monomer in the solid also revealed a shift in absorption from 3376 cm$^{-1}$ for PDI **13** to 3308 cm$^{-1}$ for **P2** characteristic of hydrogen bonding between the amides (Figure S3). From this IR data it can be concluded that the attachment of the perylene to the central polymer chain does not affect the hydrogen bonding network of the polyisocyanide. (Table S1).

**UV/Vis spectroscopy**: The absorption spectrum of **P3** in chloroform shows vibronic bands of the PDI $S_0$–$S_1$ optical transition between 400 and 600 nm (Figure 2). Compared with the spectrum of monomer **9**, the absorption spectrum of the polymer revealed a blue shifted maximum and a relatively increased oscillator strength for the 0–1 and 0–2 vibrational transitions over the 0–0 transition; this can be quantified by the ratio of the absorptions $A^{0\rightarrow0}/A^{0\rightarrow1}$ which has value of 1.66 for the monomer and 0.66 for the polymer.[24,26,27] In addition, the maxima of all vibronic bands were red shifted by 2–6 nm and a broad absorption tail was found to be present at lower energy than the 0–0 transition of monomer **9**. These spectral changes observed upon polymerization are reminiscent of weak exciton coupling interactions (strong exciton–phonon coupling) between the PDIs in H-type aggregates.[44,45] Polyisocyanides are known to adopt a $4_1$ helical structure, in which dipole–dipole interactions ($C_{1-5}$) between the $n$th and the $(n+4)$th units dominate. In such weakly coupled aggregates, excited states are grouped into vibronic bands that correspond to the single molecule vibronic lines (0–0, 0–1, etc.) in the case of vanishingly small

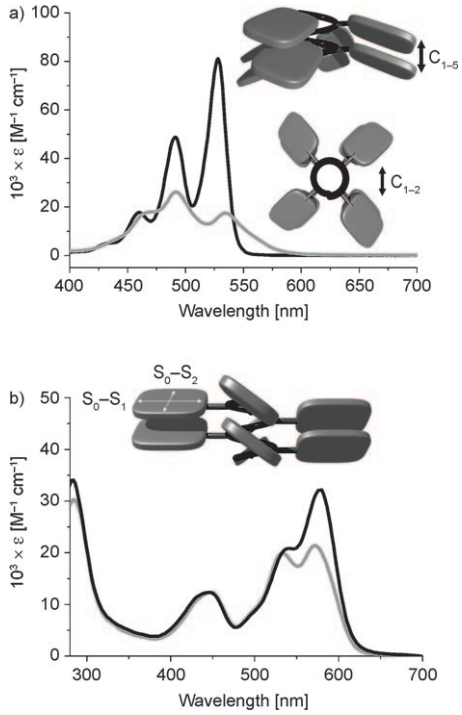


Figure 2. a) Absorption spectrum of **P3** (grey) and monomer **9** (black) ($CHCl_3$; $10^{-5}$ M). Inset: illustration of the different interactions between the PDIs in polymer **P3**. b) Absorption spectrum of **P2** (grey) and monomer **12** (black). Inset: illustration of the $S_0$–$S_1$ and $S_0$–$S_2$ transition dipoles ($CHCl_3$; $10^{-5}$ M).

  

electronic interactions. Of particular interest is the relative intensity of the $A^{0\rightarrow0}$ band as the intensity of this band diminishes with increasing exciton bandwidth and is thus a useful measure of the electronic coupling.[44–46]

The formation of exciton states resulting from intermolecular interactions leads to broader spectral features in **P3** compared to **9**. The loss of oscillator strength in the $A^{0\rightarrow0}$ band (and simultaneous increase in higher energy bands) is primarily due to the interband coupling between zero-order vibronic excitons in the $A^{0\rightarrow0}$ band with zero-order vibronic excitons in the higher energy bands ($A^{0\rightarrow1}$, $A^{0\rightarrow2}$, etc.), mediated by excitonic interactions.[47] Such interactions lead to a decrease in the $A^{0\rightarrow0}/A^{0\rightarrow1}$ ratio as well as a slightly increased spectral separation between the 0–0 and 0–1 absorption peaks. The demise of the $A^{0\rightarrow0}/A^{0\rightarrow1}$ ratio is a precursor to the more conventional blue-shifted main absorption peak characteristic of H-aggregates with much stronger excitonic coupling. The rigid red shift of the whole spectrum upon going from monomer **9** to polymer **P3** is likely due to a gas-to-crystal shift induced by aggregation (though it is possible that the weak $C_{1-2}$ interactions also contribute to a small red shift). A detailed analysis of the absorption spectrum of **P3** is provided in the modelling section.

In the absorption spectra of **P2** and **12**, besides the $S_0$–$S_1$ transition, the $S_0$–$S_2$ transition was also visible at $\lambda = 448$ nm (Figure 5). The $S_0$–$S_1$ transitions of **P2**, compared to monomer **12**, revealed relatively increased intensities of the 0–1 and 0–2 oscillations with respect to the 0–0 oscillation; $A^{0\rightarrow0}/A^{0\rightarrow1}$ equals 1.48 for the monomer and 1.07 for the polymer, suggesting (weak) electronic interactions between the chromophores.[24,26,27] In addition, a blue shift of 4 nm of the absorption maxima was detected and in contrast to **P3**, no red shifted component was visible for the $S_0$–$S_1$ transitions. For $S_0$–$S_2$ transition a tiny red shift of 2 nm was observed. The relatively increased oscillator strength for the $S_0$–$S_1$ transition in the blue is similar to observations for PDI dimers and might be indicative for H-aggregation of the PDIs, however, the absence of a red shifted component is atypical and has not been observed in the dimer model systems.[48] Besides exciton coupling, changes in the spectrum might also be caused by conformational changes induced by steric interactions between the bulky PDIs, which makes the interpretation of the absorption spectra more complex.

**CD spectroscopy**: Since the polymers adopt a helical arrangement induced by the L-alanine unit in the side arms of the polymer, circular dichroism (CD) is a powerful tool to analyze the arrangement of the chromophores in the polyisocyanopeptides.[34,49] The CD spectrum of **P3** revealed strong positive and weaker negative signals for the exciton coupled $S_0$–$S_1$ vibronic transitions between 420 and 600 nm (Figure 3). No CD signal was detected for the monomer. The CD effect is unlike any other signals observed for chiral perylene bisimides stacks and can be rationalized by considering the multiple chiral interactions in which every perylene bisimide unit is involved.[14,50] In **P3** every chromophoric unit has chiral interactions with adjacent units within the same stack ($C_{1-5}$) and with units in adjacent stacks ($C_{1-2}$) (see Figure 5), while the helicity is close to $4_1$. While the signal arising from interactions between two nearest PDIs in different stacks reflects the helicity of the polymer backbone, the one between two perylenes within the same stack originates from the helicity of the $S_0$–$S_1$ transitions within the PDI stacks.[51] The positive signal at higher wavelength, most likely originating from a positive bisignate signal, would correspond to a right handed polymer helix.[52,53] This is in agreement with the smaller positive cotton effect at 317 nm originating from the helicity in the polyimine backbone. The latter signal is similar to that observed for right handed helices of **P1** and also reflects the robustness of the isocyano-L-alanyl backbone, which is not influenced by the outer PDI substituents.[29,49,54] This robustness is also reflected by the identical CD spectra of polymer **P3** in different solvents such as, chloroform, tetrachloroethane and toluene.

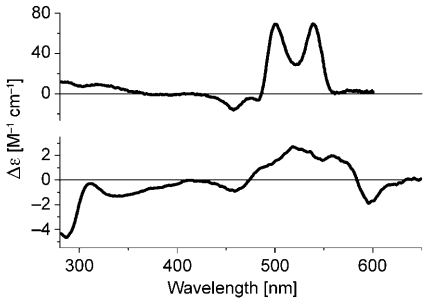


Figure 3. CD spectrum of polymer **P3** (top) and polymer **P2** (bottom) ($CHCl_3$; $10^{-5}$ M).

The CD spectrum of **P2** displayed a signal for the perylene absorptions with a lower intensity (30 times) than that observed for **P3** (Figure 3). This suggests that the PDIs in the $C_{1-4}$ geometry (Figure 2) have either a very small twist angle with respect to each other or that this angle fluctuates between positive and negative values along the stack. It is possible that the weak CD effect originates not from exciton coupling, but from induced chirality in the perylene plane; for these phenoxy substituted PDIs an excess of an *M* or *P* twist is likely to be induced by the incorporation of the PDIs in the helical polymer backbone. Such an effect has previously been observed for aggregates of similar PDIs for which a similar CD effect was observed.[50] A relatively strong signal for **P2** was visible at $\lambda = 284$ nm, preceded by a broad signal around $\lambda = 338$ nm. The signal located at 280 nm is most likely caused by chiral interactions between the phenoxy substituents, but also the imine backbone signal is expected to be present in this region. It is therefore difficult to conclude from the CD signal in this region what is the helix conformation of the polymers.

The thermal stability of the perylene-functionalized polymers **P2** and **P3** was investigated by performing temperature-dependent CD measurements. The CD signal of **P3** at $\lambda = 504$ nm in tetrachloroethane (TCE) gradually decreased in changing from −10 to 110 °C, most likely due to increased thermal motion of the perylene bisimide. The initial signal

  

was almost completely restored cooling the solution back to −10 °C, and remained the same even after five heating-cooling cycles (Figure S4).[55]

In contrast, upon heating a solution of **P2** in TCE from 20 to 110 °C all absorption, emission and CD signals decreased and were not restored upon cooling. The signal also slowly decreased in time without any heating, while this was not observed for the solution in $CH_2Cl_2$. This indicates that the conformation in TCE is thermodynamically not stable. In conclusion, these CD and DSC measurements indicate that heating of **P3** up to 110 °C does not result in irreversible changes in the polymer, reflecting the stable and thermodynamic nature of these systems.

## Modeling studies

**Morphology investigations**: As a first step in the modeling study of polyisocyanides with pendant perylene diimides, a complete morphological investigation was performed. The conformation of the polyisocyanide template in the absence of chromophores was first explored using the Dreiding force field as it is particularly suited to reproduce hydrogen bonds, which play a crucial role in the stability of the polyisocyanide backbone.[56] The torsion potential around the polymer backbone, however, is not properly accounted for by the original Dreiding force field and has been corrected against ab initio MP2 6-1G** quantum-chemical calculations. The polymer helices were built according to a "step-by-step" approach where oligomers of increasing size were grown. At each step, the lowest energy structures were retained for the generation of the larger size oligomers. From this conformational study, the most stable conformer was identified to be a right-handed helix (for an L-alanine amino acid) with an average angle of 21.3° between two successive units along the helix axis, 3.76 units per turn and a pitch length of 67.8 Å. Such a conformation was very robust against long molecular dynamics simulations at room temperature.

The predicted geometric parameters are in excellent agreement with the corresponding data extracted from a detailed spectroscopic studyof polyisocyanides substituted with porphyrin derivatives (Table 1).[34] Thus, the positioning in space of the chromophores in these helices is fixed to a large degree by the template effect enforced by the polyisocyanide core, which in turn arises mostly from the formation of an H-bonded network (Figure 4). In addition, dynamic modelling revealed that all the H-bonds point in the same direction, explaining the extremely high dipole moment of these molecules (in the range 2.8–3.6 D per repeating unit).[57] The next step of the modelling involved the grafting of PDI chromophores onto the helical polymer. The PDI molecules were linked to the backbone via a short saturated

Table 1. Comparison of the calculated (Dreiding force field) structural parameters of unsubstituted polyisocyanides with the corresponding values extracted from optical studies of polyisocyanides bearing porphyrin derivatives.[34]

| Angle between units $n$ and $n+4$ ($\beta$) [°] | Distance between units $n$ and $n+4$ ($C_{1-5}$) [Å] | Units per turn | Pitch length [Å] | |
|---|---|---|---|---|
| Dreiding | 21.3 | 4.34 | 3.76 | 67.8 |
| experiment | 22 | 4.2 | 3.75 | 68.7 |

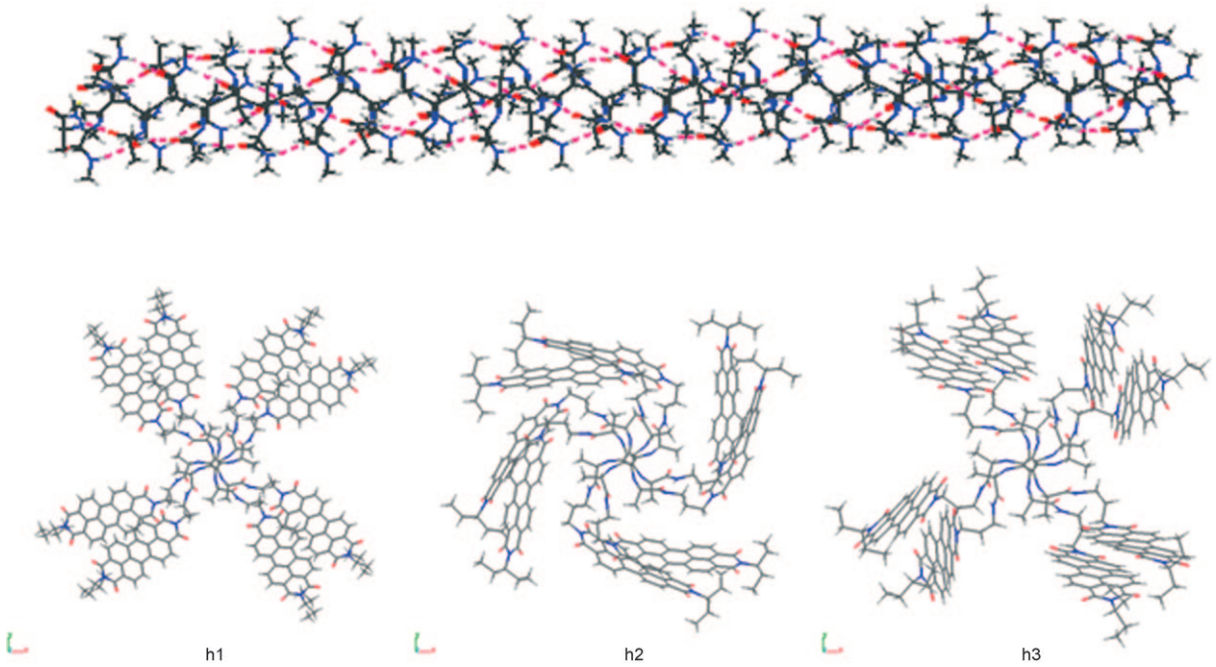


Figure 4. Most stable conformation of the unsubstituted polyisocyanide helix as obtained from Dreiding force field calculations (top). The H-bonds are indicated by dashed lines. Top view of **h1**, **h2**, and **h3** (bottom).

  

spacer that was submitted to a conformational search. Based on the local minima found for the relevant torsions, all possible helical stacks were constructed, among which the most realistic conformations based on simple steric arguments were selected for further investigations. The values of the torsion angles defining the conformation of the spacer and their combination had a considerable impact on the relative arrangement of the chromophores in the resulting 3D structures. Geometric optimizations were performed on systems of increasing complexity and converged to the identification of three local minima on the potential energy surface. To avoid finite size effects along the polymer direction, periodic boxes out of these three structures were subjected to further structural refinements. These helices, hereafter referred to as **h1**, **h2** and **h3**, differ by the relative orientation of the PDI chromophores with respect to the main axis of the polyisocyanide backbone (Figure 4). In **h1**, the PDIs are oriented with their long axis forming an angle of $\approx 60°$ with the helical direction. This is an open structure that shows the lowest density among the three helical arrangements.

The helix **h3**, in contrast to **h2**, presents a much more compact, pinetree-like structure where the PDI chromophores are lying almost down on the helical core (the average angle between the PDI main axis and the helix direction is 26°). A similarly dense structure is achieved in **h2**, although in contrast to **h3**, the chromophores are maintained in an orthogonal orientation (average angle of 94°) with respect to the helical growth direction. The interactions between the PDIs are different for all three helices. In **h1** the PDIs interact mostly via face-on interactions, while in **h2** the chromophores are lying more in an edge-on organization. In **h3** the PDI interactions also involve a cofacial arrangement, yet with translational displacement along the PDI long axes. In each of the three cases, the polymer self-organizes into a right-handed helix with 3.7–3.9 molecules per helical turn (resulting in an average rotation angle between two successive PDI along the stacking direction of $\approx 21°$ for **h1**, $\approx 24°$ for **h2** and $\approx 11°$ for **h3**). With the exception of **h3**, the angles are close to the value measured for the porphyrin-substituted polyisocyanide (22°), thus confirming that grafting of the PDI units does not perturb the structural organization of the polyisocyanide template.[34] From an energetic point of view, the potential energies calculated for these local minima indicate that **h3** is the most stable(mainly due to attractive Van der Waals interactions), followed by **h2** and **h1**.

The three local minima, identified from the geometric optimizations at 0 K then were then subjected to molecular dynamics simulations at room temperature. The aim of this study was twofold: i) it allows gauging the stability of the conformers with respect to thermal fluctuations and, in addition, ii) the snapshots extracted along the molecular dynamics (MD) run can subsequently be used to assess the influence of conformational motion on the electronic and optical properties of the polymer. A comparison between the morphologies of the various structures obtained along the MD trajectory revealed that these follow quite substantial structural changes as far as the relative arrangement of the PDI units is concerned (while the stiff helical backbone remained largely unaffected). The spacers connecting the PDI units to the carbon backbone thus allows some flexibility in the spatial positioning of the chromophores that organize into ordered domains separated by defects. This is particularly pronounced in the case of the sparse helix **h1**, which collapses into a structure similar to **h2** along the MD run. The measured angles between the PDI main axis and the helix direction indeed switched from an average value of 60° at time zero to 74° after 300 ps. The denser structures **h2** and **h3** maintained their overall organization during the full MD simulations (the corresponding rotation angles vary from 94 to 88° for **h2** and from 26 to 27° for **h3**). Thus, the morphological analysis has allowed pinpointing three structures that differ by the conformation of the arms connecting the PDI to the template and yield different relative spatial orientations of the chromophores. From the three modeled helical conformations, **h2** and **h3** appear to be the most stable conformers.[58]

## Spectroscopic investigations

The geometric structures generated from the morphology studies described above were used as input for quantum-chemical calculations of the electronic excited states (performed at the INDO/CCSD level).[59,60] The results of these calculations were in turn injected into a phenomenological Holstein model to predict the spectroscopic properties of the helical supramolecular structures, namely the optical absorption and circular dichroism spectra. A single effective high-frequency (0.17 eV) vibrational mode was included whose exciton-phonon coupling (Huang–Rhys factor of 0.6) was fitted against the absorption spectrum of an isolated PDI chromophore in solution. The model and its applications to spectroscopy have been largely described in previous works.[61,62] The polyisocyanide helices possess less than four monomer units per turn, and therefore the PDIs grafted onto the template yield four quasi-one-dimensional stacks. The absorption and CD spectra were simulated for 20-mer chains (i.e., chains formed by four 1D stacks of five molecules each); test calculations on longer oligomers yield very similar results.[63]

The comparison of the measured and simulated (from snapshots at the beginning and end of the MD run) absorption spectra for the three helical structures is shown in Figure 5. A reasonable agreement between theory and experiment is observed in all cases, with a slightly better match for helix **h1**. The spectra show the characteristic features of a weakly coupled aggregate (see above).[64] At this stage it is very difficult to rule out any structure from the comparison between measured and simulated absorption spectra, since linear absorption is not very sensitive to long-range interactions.[46]

As the nearest neighbour couplings are very similar from one conformer to another, the computed spectra are only weakly dependent on the helical conformation and on its

  

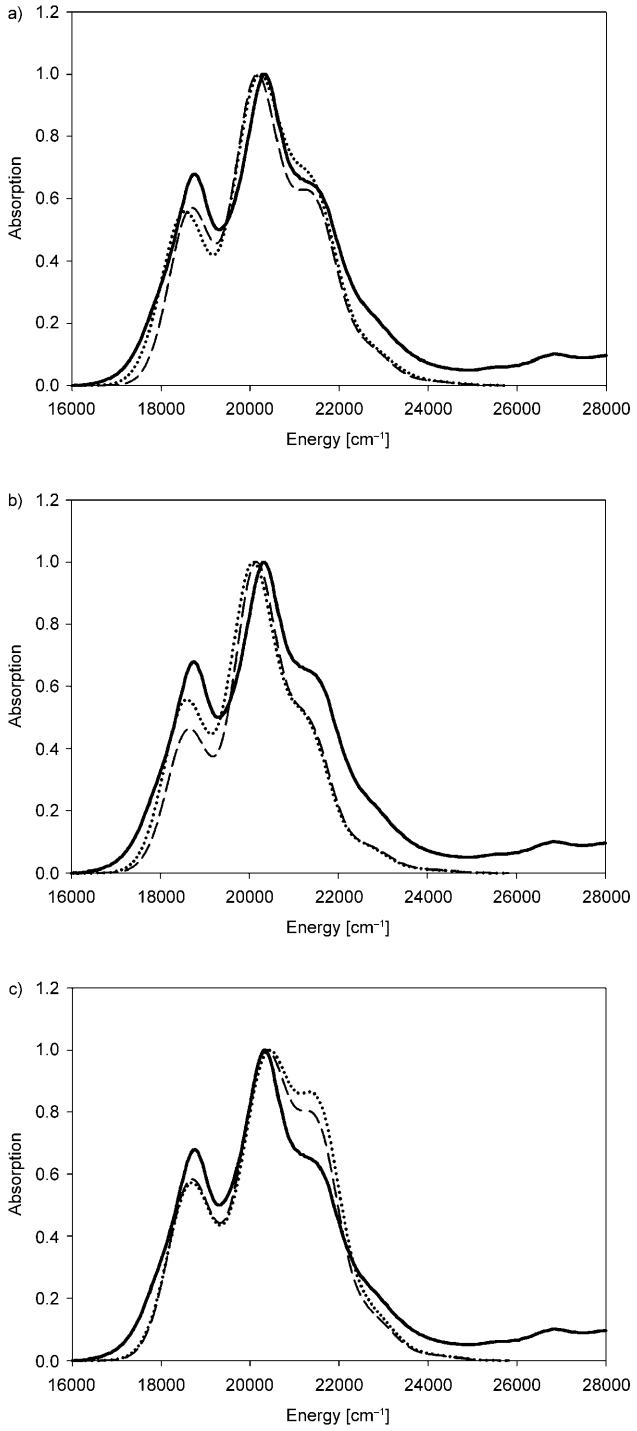


Figure 5. Theoretical absorption spectra of structures a) **h1**, b) **h2** and c) **h3**, before ($t=0$ ps, -----) and after the MD run ($t=300$ ps, •••••), overlaid to the experimental spectrum of **P3** (——) measured in a chloroform solution. Note that the theoretical spectra have been rigidly shifted to reproduce the position of the measured absorption maxima,

structural fluctuations during the MD run. This is particularly striking for **h1**, which shows very similar absorption line shapes before and after the MD simulation, despite pronounced structural reorganizations. In addition, it is also conceivable that the limiting structures considered here are, in fact, all present in solution and contribute to the overall optical properties of the polymer.

CD spectroscopy provides a more critical test for the spatial organization of the chromophores in the helical polymer as it is far more sensitive to long-range interactions than linear absorption.[65,66] When two chromophores are electronically coupled in a chiral structure, the two electronic excited states resulting from the interactions feature rotational strengths with opposite signs. Therefore, the intermolecular interactions between conjugated segments in helical conformations usually result in a double-peak signal (bisignated Cotton effect) in the CD spectrum; right-handed helices are characterized by a positive peak followed by a negative peak with increasing energy, while the reverse is true for left-handed helices. All conformers generated by the force field calculations were right-handed, at least from the mere inspection of the twisting angles between closely spaced PDI units along the four individual stacks. The experimental CD spectrum complies with this and shows the "+/-" sequence expected for a right-handed helix.

The simulated CD spectra for the three conformers, before and after the MD run are shown in Figure 6. Strikingly, **h3** shows a CD signal that is inverted with respect to **h2** and to experimental results. This is also the case for **h1** at $t=0$ ps, but the bisignated effect switches sign during the MD simulation. All individual stacks extracted from the three conformations are, however, right-handed, as proven by calculations retaining only molecules $n$, $n+4$, $n+8$, etc.

Calculation of the rotational strength for all possible PDI pairs within the full structures (not shown) revealed the presence of both positive and negative interactions. In fact, on top of the right handedness conferred by the relative positions of the chromophores within each stack, molecules belonging to different stacks also arrange according to helical structures with opposite (left) handedness. The balance between the "right" and "left" interactions depends on the conformation of the polymer chains, with only **h2** providing a qualitative match with experiment. It is interesting to see that the change in structure of **h1** evolving toward that of **h2** along the MD trajectory is accompanied by a reversal of the CD spectrum. It can be concluded from the modelling studies that the most probable conformation for these helical arrays in solution and the solid state is the architecture **h2**. This modelled architecture accounts not only for all the physical observations (UV/Vis and CD), but predicts that the polyisocyano-perylenes would be ideal polymers for exciton and electron migration. To study this we examined the photophysical behaviour of **P2** and **P3**.

**Fluorescence spectroscopy**: The fluorescence spectrum of **P3**, compared to that of monomer **9**, showed a broad structureless red shifted emission at $\lambda=625$ nm with a fluorescence quantum yield of 3.7% (in solution ($CHCl_3$) in air[67]) upon excitation at the absorption maximum at $\lambda=492$ nm (Figure 7). The low quantum yield and long fluorescence lifetime (see photophysical studies) of the emission are reminiscent of a parallel orientation of the transition dipoles

  

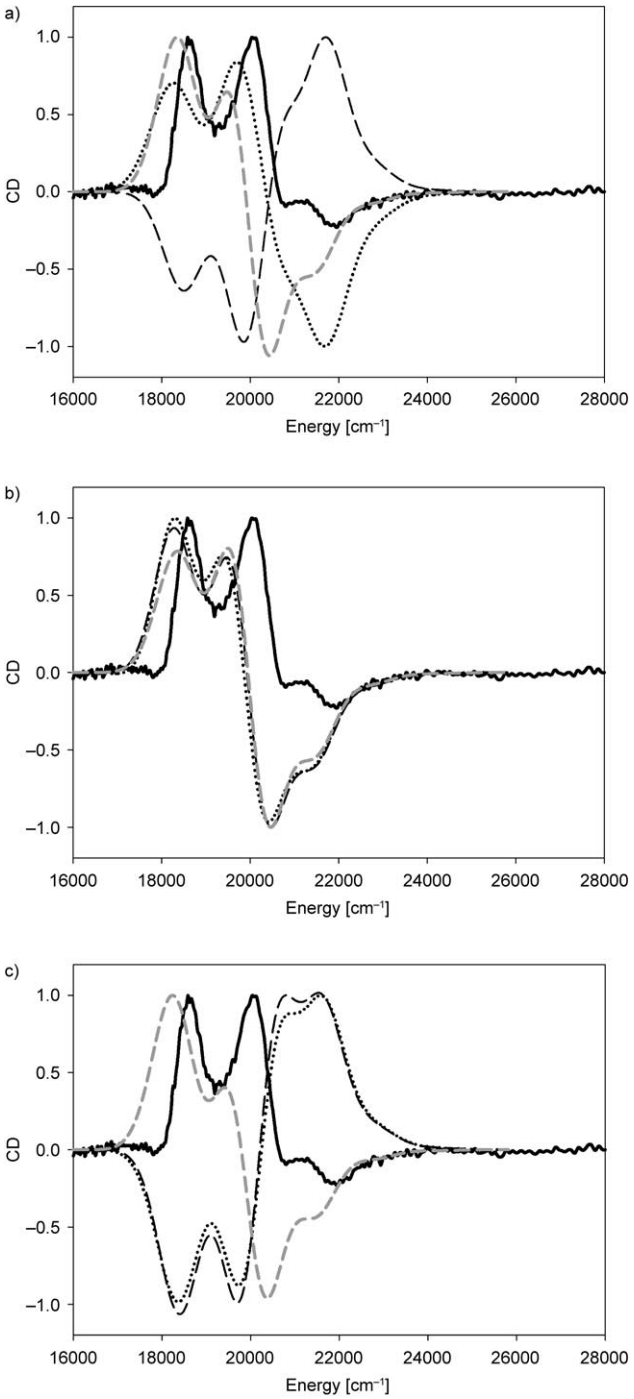


Figure 6. Theoretical CD spectra before ($t=0$ ps, -----) and after the MD run ($t=300$ ps, •••••) of structures a) **h1**, b) **h2** and c) **h3** overlaid to the experimental spectrum of **P3** (——) measured in a chloroform solution; spectra simulated for individual 1D stack -----.

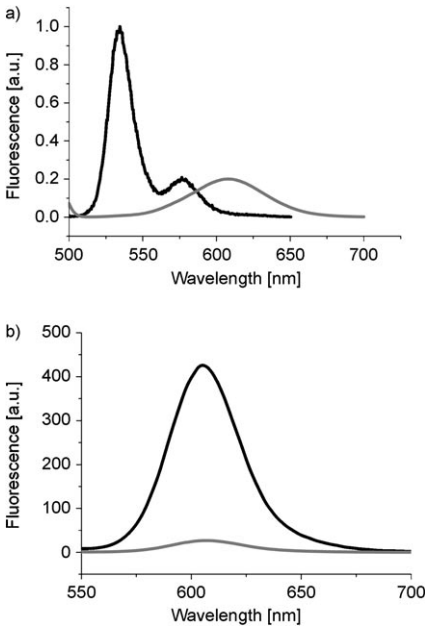


Figure 7. a) Solution fluorescence spectra of polymer **P3** (intensity ×5, grey) and monomer **9** (black) ($CHCl_3$; $10^{-6}$ M). b) Solution fluorescence spectra of polymer **P2** (grey) and PDI **12** (black) ($CHCl_3$; $10^{-6}$ M).

and are in agreement with the absorption characteristics. The featureless emission of the polymer, which is red-shifted by more than 70 nm, together with the fact that the shift in the emission spectrum is much larger than the shift in the absorption spectrum, is indicative of the formation of an intramolecular excimer-like species, although the effect of aggregate states can not be ruled out. Excimer species are formed only after excitation of monomeric species and therefore the emission, but not the absorption, is red-shifted. The chromophores in an excimer are typically 0.3–0.4 nm apart and can involve more than two chromophoric units in molecular aggregates.[35,36,68,69] The formation of excimers of aromatic hydrocarbons is restricted to a parallel cofacial configuration and confirms the conclusion that the PDIs stack in an H-aggregated fashion.

The fluorescence spectrum of **P2** has a slightly redshifted emission at $\lambda=607$ nm compared to $\lambda=605$ nm observed for the monomer. This value is comparable to the shifts in the absorption spectrum (Figure 7). The fluorescence quantum yield of **P2** amounted to 3.0% with respect to the monomer. This low quantum yield is in line with H-aggregated PDIs, however, it can also be attributed to electron transfer between the PDI and neighbouring phenoxy substituents. The emission spectra gave no evidence for excimer emission, as was observed for **P3**, which is consistent with the conclusion that the steric bulk of the phenoxy groups of the PDIs in **P2** seem to be able to prevent excimer formation.

To investigate the photophysical properties and excited state dynamics of **P3**, time-correlated single photon counting (TCSPC) and transient absorption spectroscopy were performed. The TCSPC technique (Figure 8a) revealed an extraordinarily long radiative lifetime of $\approx 24$ ns in a $CHCl_3$ solution, as compared to the usual value of 3–4 ns in the perylene monomer;[70,71] this is strongly indicative of excimer-like excited states in the polymer.[26,35,36] When the polymer was spun onto a film, the system decayed rapidly and multiexponentially due to the three dimensional energy migration in the film.

  

Polarization-sensitive transient absorption measurements of **P3** (Figure 8b) showed that the anisotropy in photo-induced absorption decays on timescales of the order of picoseconds, which is faster than in other known π-conjugated polymers, such as polythiophene.[72]

We consider that the faster energy transfer and depolarization process which take place in **P3** are due to its compact helical structure,[73] which promotes rapid exciton migration along the chiral arrangement of perylene stacks. The depolarization process is especially fast in thin films, reflecting the higher dimensionality of migration, relative to solution measurements.

The transient absorption spectra (Figure 8c–d) show ground-state absorption bleaching around $\lambda = 525$ nm, as well as a broad (from $\lambda = 550$ nm to at least $\lambda = 750$ nm) photo-induced absorption (PA) band; the latter of these being indicative of strong interactions between the chromophores.[74] The spectra obtained from both solution and film showed these features, although the shapes of the PA bands were rather different; this might be due to charge generation in the film. Furthermore, the non-linear dependence of the PA intensity on pump-fluence (Figure S5) suggests that bimolecular annihilation processes takes place in the system. Early time decay kinetics are very much faster than the ns decay rates for excitons at longer times.

High fractional changes in optical density (above ca. 1% in solution) are observed at short times showing an extremely high excitation density on chains. This suggests that the polymers are promising compounds for light-harvesting applications, such as photovoltaics[75] and thin-film transistor architectures.[76]

## Conclusion

A careful study on two novel soluble perylene-based polyisocyanopeptides performed using various experimental and computational methodologies provided unambiguous evidence that these ultrastiff polymers are ideal scaffolds for precisely organizing chromophoric arrays into functional 2D wires. The precise organization of the polymer and its side chain has been, for the first time, fully analyzed for two different polymers exposing perylene dyes. Extensive molecular modelling dynamics refines previous models, revealing a $4_1$ helix in which the chromophores overlap along the polymer backbone. The calculated and spectroscopically observed architectures predict that these unique polymers are highly favorable systems for electron transport. This was confirmed by transient absorption spectroscopy studies, which indicates extremely high exciton migration rates and charge densities. The application of these materials in thin-film transistors (TFTs) and photovoltaics is currently under study. The scaffolding approach employed here is very versatile and can be employed to dictate the spatial localization of functional groups (possessing for example, optical, electrical or catalytic activity) in pre-determined positions, paving

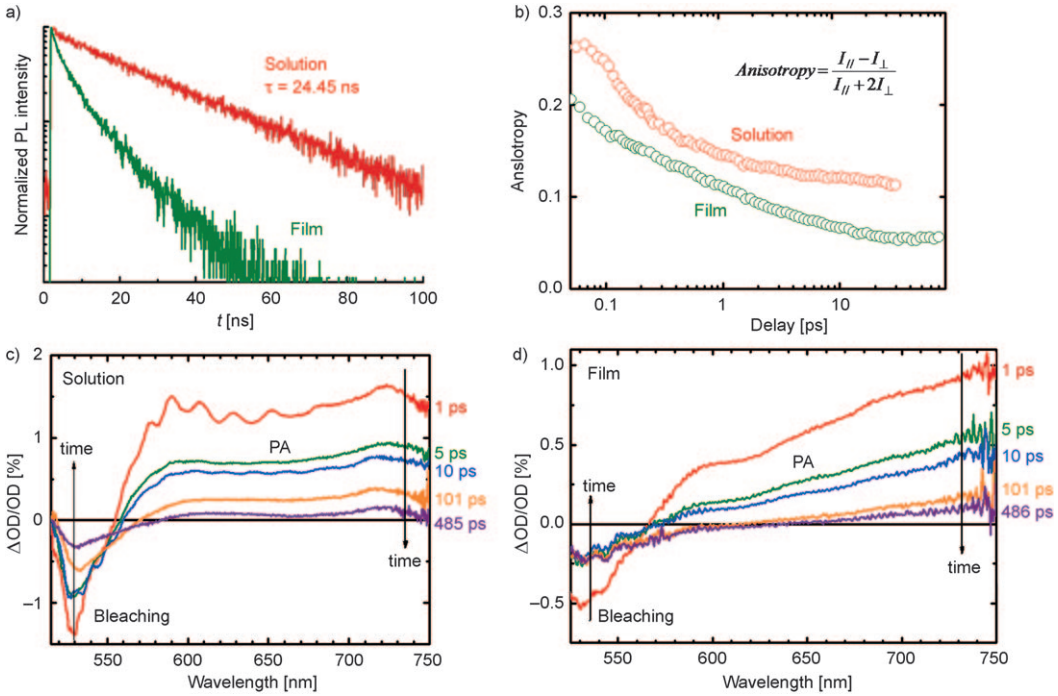


Figure 8. a) Time-resolved photoluminescence decay dynamics, measured at $\lambda = 625$ nm. b) Photo-induced absorption anisotropy measurements on **P3**, detected at 690 nm, in both film and in chloroform solution. The excitation was at 500 nm with a fluence of 424 μJ cm$^{-2}$. Transient absorption (fractional change in optical density {OD}) measurements on **P3**, being excited at 500 nm, are shown in solution (c) and in film (d). The fluences of the transient absorption measurements for the solution and film were 353 and 389 μJ cm$^{-2}$, respectively. The spectral features of bleaching and photo-induced absorption (PA), as a function of delay time, are indicated for clarity.

  

the way towards applications in various fields including optoelectronics, catalysis and medicine.

## Acknowledgement

We would like to thank B. Simons for help with AFM measurements. This work was supported by the Netherlands Organization for scientific research chemistry section (top grant for R.J.M.N and V.I.C.I, A.E.R), Nanoned STW A.E.R., the Royal Netherlands Academy for Arts and Sciences (KNAW), ESF-SONS2-SUPRAMATES and ESF-SONS-BIONICS projects, the EU through the projects Marie Curie EST-SUPER (MEST-CT-2004-008128), Marie Curie RTNs PRAIRIES (MRTN-CT-2006-035810), ForceTool (NMP4-CT-2004-013684), the ERA-Chemistry project SurConFold and the Regione Emilia-Romagna PRIITT Nanofaber Net-Lab. C.E.F. thanks the Leverhulme Trust (UK) for an "Early Career Fellowship".The work at Temple is supported by the National Science Foundation, grant #DMR-0606028. The work in Mons is partly supported by the Interuniversity Attraction Pole program of the Belgian Federal Science Policy Office (PAI 6/27) and by FNRS-FRFC. D.B. is research director of FNRS. S.T. acknowledges a grant from Fonds pour la Formation à la Recherche dans l'Industrie et dans l'Agriculture (FRIA).

[1] C. D. Dimitrakopoulos and P. R. L. Malenfant, *Adv. Mater.* **2002**, *14*, 99–117.
[2] C. W. Struijk, A. B. Sieval, J. E. J. Dakhorst, M. van Dijk, P. Kimkes, R. B. M. Koehorst, H. Donker, T. J. Schaafsma, S. J. Picken, A. M. van de Craats, J. M. Warman, H. Zuilhof, E. J. R. Sudholter, *J. Am. Chem. Soc.* **2000**, *122*, 11057–11066.
[3] B. A. Gregg, J. Sprague, M. W. Peterson, *J. Phys. Chem. B* **1997**, *101*, 5362–5369.
[4] Z. J. Chen, M. G. Debije, T. Debaerdemaeker, P. Osswald, F. Würthner, *ChemPhysChem* **2004**, *5*, 137–140.
[5] R. J. Chesterfield, J. C. McKeen, C. R. Newman, P. C. Ewbank, D. A. da Silva, J. L. Bredas, L. L. Miller, K. R. Mann, C. D. Frisbie, *J. Phys. Chem. B* **2004**, *108*, 19281–19292.
[6] P. R. L. Malenfant, C. D. Dimitrakopoulos, J. D. Gelorme, L. L. Kosbar, T. O. Graham, A. Curioni and W. Andreoni, *Appl. Phys. Lett.* **2002**, *80*, 2517–2519.
[7] M. J. Ahrens, L. E. Sinks, B. Rybtchinski, W. H. Liu, B. A. Jones, J. M. Giaimo, A. V. Gusev, A. J. Goshe, D. M. Tiede, M. R. Wasielewski, *J. Am. Chem. Soc.* **2004**, *126*, 8284–8294.
[8] K. Balakrishnan, A. Datar, T. Naddo, J. L. Huang, R. Oitker, M. Yen, J. C. Zhao, L. Zang, *J. Am. Chem. Soc.* **2006**, *128*, 7390–7398.
[9] D. Franke, M. Vos, M. Antonietti, N. A. J. M. Sommerdijk, C. F. J. Faul, *Chem. Mater.* **2006**, *18*, 1839–1847.
[10] J. M. Giaimo, A. V. Gusev, M. R. Wasielewski, *J. Am. Chem. Soc.* **2002**, *124*, 8530–8531.
[11] Y. Guan, Y. Zakrevskyy, J. Stumpe, M. Antonietti, C. F. J. Faul, *Chem. Commun.* **2003**, 894–895.
[12] K. Sugiyasu, N. Fujita, S. Shinkai, *Angew. Chem.* **2004**, *116*, 1249–1253; *Angew. Chem. Int. Ed.* **2004**, *43*, 1229–1233.
[13] M. J. Tauber, R. F. Kelley, J. M. Giaimo, B. Rybtchinski, M. R. Wasielewski, *J. Am. Chem. Soc.* **2006**, *128*, 1782–1783.
[14] C. Thalacker, F. Würthner, *Adv. Funct. Mater.* **2002**, *12*, 209–218.
[15] Y. Zakrevskyy, C. F. J. Faul, Y. Guan, J. Stumpe, *Adv. Funct. Mater.* **2004**, *14*, 835–841.
[16] V. Palermo, A. Liscio, D. Gentilini, F. Nolde, K. Müllen, P. Samori, *Small* **2007**, *3*, 161–167.
[17] G. De Luca, A. Liscio, P. Maccagnani, F. Nolde, V. Palermo, K. Müllen, P. Samori, *Adv. Funct. Mater.* **2007**, *17*, 3791–3798.
[18] A. Liscio, G. De Luca, F. Nolde, V. Palermo, K. Muellen, P. Samori, *J. Am. Chem. Soc.* **2008**, *130*, 780–781.
[19] S. G. Liu, G. D. Sui, R. A. Cormier, R. M. Leblanc, B. A. Gregg, *J. Phys. Chem. B* **2002**, *106*, 1307–1315.
[20] F. Würthner, Z. J. Chen, V. Dehm, V. Stepanenko, *Chem. Commun.* **2006**, 1188–1190.
[21] F. Würthner, C. Thalacker, S. Diele, C. Tschierske, *Chem. Eur. J.* **2001**, *7*, 2245–2253.
[22] J. J. Han, W. Wang, A. D. Q. Li, *J. Am. Chem. Soc.* **2006**, *128*, 672–673.
[23] C. Hippius, F. Schlosser, M. O. Vysotsky, V. Bohmer, F. Würthner, *J. Am. Chem. Soc.* **2006**, *128*, 3870–3871.
[24] A. D. Q. Li, W. Wang, L. Q. Wang, *Chem. Eur. J.* **2003**, *9*, 4594–4601.
[25] E. E. Neuteboom, R. A. J. Janssen, E. W. Meijer, *Synth. Met.* **2001**, *121*, 1283–1284.
[26] E. E. Neuteboom, S. C. J. Meskers, E. W. Meijer, R. A. J. Janssen, *Macromol. Chem. Phys.* **2004**, *205*, 217–222.
[27] W. Wang, L. S. Li, G. Helms, H. H. Zhou, A. D. Q. Li, *J. Am. Chem. Soc.* **2003**, *125*, 1120–1121.
[28] W. Wang, W. Wan, H. H. Zhou, S. Q. Niu, A. D. Q. Li, *J. Am. Chem. Soc.* **2003**, *125*, 5248–5249.
[29] J. J. L. M. Cornelissen, A. E. Rowan, R. J. M. Nolte, N. A. J. M. Sommerdijk, *Chem. Rev.* **2001**, *101*, 4039–4070.
[30] R. J. M. Nolte, *Chem. Soc. Rev.* **1994**, *23*, 11–19.
[31] Y. Okamoto, T. Nakano, *Chem. Rev.* **1994**, *94*, 349–372.
[32] M. Suginome, Y. Ito, *Adv. Polym. Sci.* **2004**, *171*, 77–136.
[33] D. M. Vriezema, J. Hoogboom, K. Velonia, K. Takazawa, P. C. M. Christianen, J. C. Maan, A. E. Rowan, R. J. M. Nolte, *Angew. Chem.* **2003**, *115*, 796–800; *Angew. Chem. Int. Ed.* **2003**, *42*, 772–776.
[34] P. A. J. de Witte, M. Castriciano, J. J. L. M. Cornelissen, L. M. Scolaro, R. J. M. Nolte, A. E. Rowan, *Chem. Eur. J.* **2003**, *9*, 1775–1781.
[35] P. A. J. de Witte, J. Hernando, E. E. Neuteboom, E. M. H. P. van Dijk, S. C. J. Meskers, R. A. J. Janssen, N. F. van Hulst, R. J. M. Nolte, M. F. Garcia-Parajo, A. E. Rowan, *J. Phys. Chem. B* **2006**, *110*, 7803–7812.
[36] J. Hernando, P. A. J. de Witte, E. M. H. P. van Dijk, J. Korterik, R. J. M. Nolte, A. E. Rowan, M. F. Garcia-Parajo, N. F. van Hulst, *Angew. Chem.* **2004**, *116*, 4137–4141; *Angew. Chem. Int. Ed.* **2004**, *43*, 4045–4049.
[37] P. Samori, C. Ecker, I. Gossl, P. A. J. de Witte, J. J. L. M. Cornelissen, G. A. Metselaar, M. B. J. Otten, A. E. Rowan, R. J. M. Nolte, J. P. Rabe, *Macromolecules* **2002**, *35*, 5290–5294.
[38] J. J. L. M. Cornelissen, W. S. Graswinckel, P. J. H. M. Adams, G. H. Nachtegaal, A. P. M. Kentgens, N. A. J. M. Sommerdijk, R. J. M. Nolte, *J. Polym. Sci. Part A-1 Polym. Chem.* **2001**, *39*, 4255–4264.
[39] P. C. J. Kamer, R. J. M. Nolte, W. Drenth, *J. Am. Chem. Soc.* **1988**, *110*, 6818–6825.
[40] S. A. Prokhorova, S. S. Sheiko, M. Moller, C. H. Ahn, V. Percec, *Macromol. Rapid Commun.* **1998**, *19*, 359–366.
[41] J. J. Cornelissen, J. J. Donners, R. de Gelder, W. S. Graswinckel, G. A. Metselaar, A. E. Rowan, N. A. Sommerdijk, R. J. Nolte, *Science* **2001**, *293*, 676–680.
[42] J. Cornelissen, W. S. Graswinckel, A. E. Rowan, N. Sommerdijk, R. J. M. Nolte, *J. Polym. Sci. Part A-1 Polym. Chem.* **2003**, *41*, 1725–1736.
[43] L. Bellamy, *The Infra Red Spectra of Complex Molecules*, Springer, Heidelberg, **1975**.
[44] F. C. Spano, *J. Chem. Phys.* **2005**, *122*, 234701.
[45] F. C. Spano, *J. Chem. Phys.* **2007**, *126*, 159901.
[46] F. C. Spano, S. C. J. Meskers, E. Hennebicq, D. Beljonne, *J. Am. Chem. Soc.* **2007**, *129*, 7044–7054.
[47] F. C. Spano, *Chem. Phys.* **2006**, *325*, 22–35.
[48] T. van der Boom, R. T. Hayes, Y. Y. Zhao, P. J. Bushard, E. A. Weiss, M. R. Wasielewski, *J. Am. Chem. Soc.* **2002**, *124*, 9582–9590.
[49] J. J. L. M. Cornelissen, N. A. J. M. Sommerdijk, R. J. M. Nolte, *Macromol. Chem. Phys.* **2002**, *203*, 1625–1630.
[50] F. Würthner, Z. J. Chen, F. J. M. Hoeben, P. Osswald, C. C. You, P. Jonkheijm, J. von Herrikhuyzen, A. P. H. J. Schenning, P. P. A. M. van der Schoot, E. W. Meijer, E. H. A. Beckers, S. C. J. Meskers, R. A. J. Janssen, *J. Am. Chem. Soc.* **2004**, *126*, 10611–10618.
[51] M. Kasha, H. Rawls, M. El-Bayoumi, *Pure Appl. Chem.* **1965**, *11*, 371.

  

[52] N. Harada, K. Nakanishi, *Circular Dichroism Spectroscopy. Exciton Coupling in Organic Stereochemistry*, University Science Books, Mill Valley, **1983**.
[53] N. Harada, K. Nakanish, *Acc. Chem. Res.* **1972**, *5*, 257–263.
[54] G. A. Metselaar, J. J. L. M. Cornelissen, A. E. Rowan, R. J. M. Nolte, *Angew. Chem.* **2005**, *117*, 2026–2029; *Angew. Chem. Int. Ed.* **2005**, *44*, 1990–1993.
[55] After one week in tetrachloroethane solution no changes in the CD spectrum were observed, however, the fluorescence spectrum revealed a small monomer like signal (<1.5% monomer), which slowly became stronger in time. The monomer-like emission might be the result of the unwinding of the helix at its terminals or slow decomposition of the polymers at its terminals, because of reaction of the polyimide backbone with carbene- or radical-like species in solution. In the solid state the polymer is very stable over periods of up to 2 years. Differential scanning calorimetry (DSC) showed an endothermic peak at 85 °C in the heating trace with a corresponding exothermic peak at 58 °C in the cooling trace, which can be attributed to the melting and crystallization of the alkyl tails in the periphery of the polymer, respectively. (Figure S4).
[56] S. L. Mayo, B. D. Olafson, W. A. Goddard, *J. Phys. Chem.* **1990**, *94*, 8897–8909.
[57] M. Kauranen, T. Verbiest, C. Boutton, M. N. Teerenstra, K. Clays, A. J. Schouten, R. J. M. Nolte, A. Persoons, *Science* **1995**, *270*, 966–969.
[58] The calculations have been done in gas phase, hence the more collapsed conformation is also the most stable. Because solvent effects are not taken into account, we have not ruled out stable structures on the basis of the sole energetic argument. Absorption and CD spectra have been done for a number of conformers and the comparison to experiment allowed us to identity the most likely conformations in solution.
[59] J. Ridley, M. Zerner, *Theor. Chim. Acta* **1973**, *32*, 111–134.
[60] Z. Shuai, J. L. Bredas, *Phys. Rev. B* **2000**, *62*, 15452–15460.
[61] F. C. Spano, *Annu. Rev. Phys. Chem.* **2006**, *57*, 217–243.
[62] H. Sun, Z. Zhao, F. C. Spano, D. Beljonne, J. Cornil, Z. Shuai, J. L. Bredas, *Adv. Mater.* **2003**, *15*, 818–822.
[63] For each chain, the ground-state geometries of the individual chromophores were extracted from the full helical structures and single point INDO/CCSD calculations were performed on the H-adjusted molecules. The obtained vertical excitation energies and excitonic couplings (computed within the transition density approach) were then used to solve the Holstein Hamiltonian within the two-particle approximation.(see refs. [61,62])
[64] The low-energy shoulder corresponds to the purely electronic 0–0 transition of the individual molecule and its relative intensity, in comparison to the higher-energy phonon sidebands, is sensitive to the magnitude of the excitonic couplings. The couplings are all in the range of 400–500 $cm^{-1}$ for the nearest neighbor interactions and significantly smaller than the geometric relaxation energy ($0.6 \times 0.17\ eV = 823\ cm^{-1}$).
[65] F. C. Spano, S. C. J. Meskers, E. Hennebicq, D. Beljonne, *J. Chem. Phys.* **2008**, *129*, 024704.
[66] F. C. Spano, Z. Zhao and S. C. J. Meskers, *J. Chem. Phys.* **2004**, *120*, 10594–10604.
[67] *A Guide to Recording Fluorescence Quantum Yields, Vol. A Guide to Recording Fluorescence Quantum Yields*, http://www.jobinyvon.com/usadivisions/fluorescence/applications/quantumyieldstrad.pdf.
[68] R. Katoh, S. Sinha, S. Murata, M. Tachiya, *J. Photochem. Photobiol A* **2001**, *145*, 23–34.
[69] M. Masuko, H. Ohtani, K. Ebata, A. Shimadzu, *Nucleic Acids Res.* **1998**, *26*, 5409–5416.
[70] P. B. Bisht, K. Fukuda, S. Hirayama, *Chem. Phys. Lett.* **1996**, *258*, 71–79.
[71] W. E. Ford, P. V. Kamat, *J. Phys. Chem.* **1987**, *91*, 6373–6380.
[72] S. Westenhoff, C. Daniel, R. H. Friend, C. Silva, V. Sundstrom, A. Yartsev, *J. Chem. Phys.* **2005**, *122*, 094903.
[73] C. Daniel, S. Westenhoff, F. Makereel, R. H. Friend, D. Beljonne, L. M. Herz, C. Silva, *J. Phys. Chem. C* **2007**, *111*, 19111–19119.
[74] C. Silva, D. M. Russell, M. A. Stevens, J. D. Mackenzie, S. Setayesh, K. Müllen, R. H. Friend, *Chem. Phys. Lett.* **2000**, *319*, 494–500.
[75] V. Palermo, M. Otten, A. Liscio, E. Schwartz, P. de Witte, M. A. Castriciano, M. M. Wienk, F. Nolde, G. De Luca, J. J. L. M. Cornelissen, R. A. J. Janssen, K. Müllen, A. E. Rowan, R. J. M. Nolte, P. Samorì, *J. Am. Chem. Soc.* **2008**, *130*, 14605–14614.
[76] C. E. Finlayson, R. H. Friend, M. B. J. Otten, E. Schwartz, J. J. L. M. Cornelissen, R. J. M. Nolte, A. E. Rowan, P. Samorì, V. Palermo, A. Liscio, K. Peneva, K. Müllen, S. Trapani, D. Beljonne, *Adv. Funct. Mater.* **2008**, *18*, 3947–3955.

Received: August 22, 2008
Published online: January 28, 2009

  